

Search for Charmless $B \rightarrow VV$ Decays

R. Godang,¹ G. Bonvicini,² D. Cinabro,² M. Dubrovin,² S. McGee,² G. J. Zhou,² A. Bornheim,³ E. Lipeles,³ S. P. Pappas,³ M. Schmidtler,³ A. Shapiro,³ W. M. Sun,³ A. J. Weinstein,³ D. E. Jaffe,⁴ G. Masek,⁴ H. P. Paar,⁴ D. M. Asner,⁵ A. Eppich,⁵ T. S. Hill,⁵ R. J. Morrison,⁵ R. A. Briere,⁶ G. P. Chen,⁶ T. Ferguson,⁶ H. Vogel,⁶ A. Gritsan,⁷ J. P. Alexander,⁸ R. Baker,⁸ C. Bebek,⁸ B. E. Berger,⁸ K. Berkelman,⁸ F. Blanc,⁸ V. Boisvert,⁸ D. G. Cassel,⁸ P. S. Drell,⁸ J. E. Duboscq,⁸ K. M. Ecklund,⁸ R. Ehrlich,⁸ A. D. Foland,⁸ P. Gaidarev,⁸ L. Gibbons,⁸ B. Gittelman,⁸ S. W. Gray,⁸ D. L. Hartill,⁸ B. K. Heltsley,⁸ P. I. Hopman,⁸ L. Hsu,⁸ C. D. Jones,⁸ J. Kandaswamy,⁸ D. L. Kreinick,⁸ M. Lohner,⁸ A. Magerkurth,⁸ T. O. Meyer,⁸ N. B. Mistry,⁸ E. Nordberg,⁸ M. Palmer,⁸ J. R. Patterson,⁸ D. Peterson,⁸ D. Riley,⁸ A. Romano,⁸ J. G. Thayer,⁸ D. Urner,⁸ B. Valant-Spaight,⁸ G. Viehhauser,⁸ A. Warburton,⁸ P. Avery,⁹ C. Prescott,⁹ A. I. Rubiera,⁹ H. Stoeck,⁹ J. Yelton,⁹ G. Brandenburg,¹⁰ A. Ershov,¹⁰ D. Y.-J. Kim,¹⁰ R. Wilson,¹⁰ T. Bergfeld,¹¹ B. I. Eisenstein,¹¹ J. Ernst,¹¹ G. E. Gladding,¹¹ G. D. Gollin,¹¹ R. M. Hans,¹¹ E. Johnson,¹¹ I. Karliner,¹¹ M. A. Marsh,¹¹ C. Plager,¹¹ C. Sedlack,¹¹ M. Selen,¹¹ J. J. Thaler,¹¹ J. Williams,¹¹ K. W. Edwards,¹² R. Janicek,¹³ P. M. Patel,¹³ A. J. Sadoff,¹⁴ R. Ammar,¹⁵ A. Bean,¹⁵ D. Besson,¹⁵ X. Zhao,¹⁵ S. Anderson,¹⁶ V. V. Frolov,¹⁶ Y. Kubota,¹⁶ S. J. Lee,¹⁶ R. Mahapatra,¹⁶ J. J. O'Neill,¹⁶ R. Poling,¹⁶ T. Riehle,¹⁶ A. Smith,¹⁶ C. J. Stepaniak,¹⁶ J. Urheim,¹⁶ S. Ahmed,¹⁷ M. S. Alam,¹⁷ S. B. Athar,¹⁷ L. Jian,¹⁷ L. Ling,¹⁷ M. Saleem,¹⁷ S. Timm,¹⁷ F. Wappler,¹⁷ A. Anastassov,¹⁸ E. Eckhart,¹⁸ K. K. Gan,¹⁸ C. Gwon,¹⁸ T. Hart,¹⁸ K. Honscheid,¹⁸ D. Hufnagel,¹⁸ H. Kagan,¹⁸ R. Kass,¹⁸ T. K. Pedlar,¹⁸ H. Schwarthoff,¹⁸ J. B. Thayer,¹⁸ E. von Toerne,¹⁸ M. M. Zoeller,¹⁸ S. J. Richichi,¹⁹ H. Severini,¹⁹ P. Skubic,¹⁹ A. Undrus,¹⁹ V. Savinov,²⁰ S. Chen,²¹ J. Fast,²¹ J. W. Hinson,²¹ J. Lee,²¹ D. H. Miller,²¹ V. Pavlunin,²¹ E. I. Shibata,²¹ I. P. J. Shipsey,²¹ D. Cronin-Hennessy,²² A. L. Lyon,²² E. H. Thorndike,²² T. E. Coan,²³ V. Fadeyev,²³ Y. S. Gao,²³ Y. Maravin,²³ I. Narsky,²³ R. Stroynowski,²³ J. Ye,²³ T. Wlodek,²³ M. Artuso,²⁴ R. Ayad,²⁴ C. Boulahouache,²⁴ K. Bukin,²⁴ E. Dambasuren,²⁴ G. Majumder,²⁴ G. C. Moneti,²⁴ R. Mountain,²⁴ S. Schuh,²⁴ T. Skwarnicki,²⁴ S. Stone,²⁴ J. C. Wang,²⁴ A. Wolf,²⁴ J. Wu,²⁴ S. Kopp,²⁵ M. Kostin,²⁵ A. H. Mahmood,²⁶ S. E. Csorna,²⁷ I. Danko,²⁷ K. W. McLean,²⁷ and Z. Xu²⁷

(CLEO Collaboration)

¹Virginia Polytechnic Institute and State University, Blacksburg, Virginia 24061

²Wayne State University, Detroit, Michigan 48202

³California Institute of Technology, Pasadena, California 91125

⁴University of California, San Diego, La Jolla, California 92093

⁵University of California, Santa Barbara, California 93106

⁶Carnegie Mellon University, Pittsburgh, Pennsylvania 15213

⁷University of Colorado, Boulder, Colorado 80309-0390

⁸Cornell University, Ithaca, New York 14853

⁹University of Florida, Gainesville, Florida 32611

¹⁰Harvard University, Cambridge, Massachusetts 02138

¹¹University of Illinois, Urbana-Champaign, Illinois 61801

¹²Carleton University, Ottawa, Ontario, Canada K1S 5B6
and the Institute of Particle Physics, Canada

¹³McGill University, Montréal, Québec, Canada H3A 2T8
and the Institute of Particle Physics, Canada

¹⁴Ithaca College, Ithaca, New York 14850

¹⁵University of Kansas, Lawrence, Kansas 66045

¹⁶University of Minnesota, Minneapolis, Minnesota 55455

¹⁷State University of New York at Albany, Albany, New York 12222

¹⁸Ohio State University, Columbus, Ohio 43210

¹⁹University of Oklahoma, Norman, Oklahoma 73019

²⁰University of Pittsburgh, Pittsburgh, Pennsylvania 15260

²¹Purdue University, West Lafayette, Indiana 47907

²²University of Rochester, Rochester, New York 14627

²³Southern Methodist University, Dallas, Texas 75275

²⁴Syracuse University, Syracuse, New York 13244

²⁵University of Texas, Austin, Texas 78712

²⁶University of Texas—Pan American, Edinburg, Texas 78539

²⁷Vanderbilt University, Nashville, Tennessee 37235

(Received 4 January 2001; published 27 December 2001)

We have studied two-body charmless decays of the B meson into the final states $\rho^0\rho^0$, $K^{*0}\rho^0$, $K^{*0}K^{*0}$, $K^{*0}\bar{K}^{*0}$, $K^{*+}\rho^0$, $K^{*+}\bar{K}^{*0}$, and $K^{*+}K^{*-}$ using only decay modes with charged daughter particles. Using 9.7×10^6 $B\bar{B}$ pairs collected with the CLEO detector, we place 90% confidence level upper limits on the branching fractions $(1.4\text{--}14.1) \times 10^{-5}$, depending on final state and polarization.

DOI: 10.1103/PhysRevLett.88.021802

PACS numbers: 13.25.Hw, 14.40.Nd

In the standard model, CP violation is introduced by the complex phase in the Cabibbo-Kobayashi-Maskawa quark-mixing matrix. The experimental study of CKM phases will probe the standard model description of CP violation. This may provide a window to new physics. In particular, it has been suggested [1] that we may construct a relationship between charmless $B \rightarrow VV$ decays that may lead to the extraction of the angle α . Earlier observations of rare charmless decay modes at CLEO include $B \rightarrow K\pi$, $\pi\pi$, ηK , $\rho\pi$, $\eta'K$, ηK^* , and $\omega\pi$ [2]. It is natural to extend our search toward other rare charmless B decays.

In this Letter, we present results of searches for B meson decays into the vector mesons ρ^0 , K^{*0} , and K^{*+} . The decays are dominated by the $b \rightarrow u$ tree-level and $b \rightarrow dg$ penguin processes, though other mechanisms may also contribute [3].

The data used in this analysis were collected by the CLEO detector [4] at the Cornell Electron Storage Ring (CESR). The data consist of an integrated luminosity of 9.1 fb^{-1} at the $Y(4S)$ resonance, corresponding to 9.7×10^6 $B\bar{B}$ events. To determine backgrounds due to nonresonant $e^+e^- \rightarrow q\bar{q}$ process, we also collected 4.6 fb^{-1} of continuum data at energies just below the $Y(4S)$ resonance.

The CLEO detector has 67 tracking layers and a CsI electromagnetic calorimeter that provides efficient π^0 reconstruction, all operating within a 1.5 T superconducting solenoid. The central tracking system, consisting of an inner 6-layer straw tube precision tracker, a 10-layer vertex drift chamber, and a 51-layer main drift chamber, provides a measurement of momenta of charged particles and the vertex position of decaying K_S . It also measures the specific ionization loss, dE/dx , which is used for particle identification. The precision tracker was replaced by a silicon vertex detector for the latter 65% of data taking. Muons are identified using proportional counters placed at various depths in the steel return yoke of the magnet.

B candidates are selected by straightforward criteria based on energy-momentum conservation and event shape. Simulations of the signal and backgrounds are used to refine these criteria and to determine their effectiveness.

The $B \rightarrow VV$ decays are reconstructed through the decay channels $B^0 \rightarrow \rho^0\rho^0$, $B^0 \rightarrow K^{*0}\rho^0$, $B^0 \rightarrow K^{*0}K^{*0}$, $B^0 \rightarrow K^{*0}\bar{K}^{*0}$, $B^+ \rightarrow K^{*+}\rho^0$, $B^+ \rightarrow K^{*+}\bar{K}^{*0}$, and $B^0 \rightarrow K^{*+}K^{*-}$. We form ρ^0 candidates from $\pi^+\pi^-$ pairs with an invariant mass within $150 \text{ MeV}/c^2$ of the nominal ρ^0 mass. $K^{*0}/\bar{K}^{*0}/K^{*\pm}$ candidates are selected from $K^\pm\pi^\mp/K_S^0\pi^\pm$ pairs within $50 \text{ MeV}/c^2$ of the nominal K^* mass.

Charged tracks are selected by requiring them to pass quality criteria and must be consistent with production from the primary interaction point (except for pions from K_S^0 decays). The measured specific ionization (dE/dx) of charged kaon and pion candidates is required to be within 3.0σ (standard deviation) of their most probable values. We reject electrons based on dE/dx and the ratio of the track momentum to the associated shower energy in the CsI calorimeter. We reject muons by requiring that the tracks not penetrate the steel absorber past a depth of 3 nuclear interaction lengths. The K_S^0 is selected by requiring a decay vertex displaced from the primary interaction point and an invariant mass within $10 \text{ MeV}/c^2$ of the K_S^0 mass.

Fully reconstructed B mesons are selected on the basis of the beam-constrained mass of the candidate, $M_B = \sqrt{E_{\text{beam}}^2 - P_{\text{reconstructed}}^2}$, and the difference between the reconstructed and beam energies, $\Delta E = E_{\text{reconstructed}} - E_{\text{beam}}$. ΔE is sensitive to missing or extra particles in the B candidate, as well as incorrect assignment of particle masses. For the fully reconstructed B meson decays in this analysis, the M_B distribution peaks at $5.28 \text{ GeV}/c^2$ with a resolution ranging between $2.2\text{--}2.6 \text{ MeV}/c^2$, and ΔE peaks at zero GeV with a resolution ranging from $16\text{--}27 \text{ MeV}$. Candidates are accepted for further analysis if ΔE and M_B are within a signal region $\pm 2\sigma$ around the central signal values for all channels (except $K^{*+}K^{*-}$ where a larger $\pm 2.8\sigma$ region of M_B is used since this involves two K_S^0 's and is therefore relatively clean).

The backgrounds consist primarily of continuum events from $e^+e^- \rightarrow q\bar{q}$ ($q = u, d, s, c$) with a 10–15% contribution from B decays, and are estimated from a combination of off-resonance data and $b \rightarrow c$ Monte Carlo. Event-shape variables can be used to discriminate against the jetlike continuum events since B mesons are produced nearly at rest. Accordingly, we select only events with $R_2 < 0.5$, where R_2 is the ratio of the second to zeroth Fox-Wolfram moments of the event [5]. In continuum events, momentum conservation aligns the thrust axis of the B candidate with that of the rest of the event while they are almost uncorrelated in $B\bar{B}$ events. This allows additional suppression of continuum by restricting $|\cos\theta_{tt}|$, the angle between the two axes. We require $|\cos\theta_{tt}| < 0.7$ for all decay modes, except for $K^{*+}K^{*-}$, where we use $|\cos\theta_{tt}| < 0.9$.

The four selection criteria discussed above, on M_B , ΔE , R_2 , and $\cos\theta_{tt}$, determine the signal efficiency (ϵ) for each mode. We measure this efficiency using Monte Carlo simulation for each of the 3 possible helicity states of the decay products: 00, $-1-1$ and $+1+1$. Our study

indicates that the 00 helicity has slightly lower efficiency than the 11 helicities, since it results in more low momentum charged pion and kaon tracks from the B decay chain, for which the detector has a lower acceptance. In addition, the 00 state will tend to align the vector decay products leading to a higher average R_2 , also decreasing the efficiency. We give separate results assuming the signal is 100% 00 helicity or 100% 11 helicity. For any assumed helicity distribution of signal events in the data sample, upper limits can be obtained by linear interpolation.

We find significant double counting of events in the $K^{*0}\rho^0$ channel, caused in most cases by the K/π ambiguity in the $K^{*0} \rightarrow K^+\pi^-$ subdecay. In the final results we count only one entry for each event. We also consider the possibility of crossfeed between different channels of $B \rightarrow VV$ decays. Neglecting the contribution from the forbidden decay mode $B \rightarrow K^{*0}K^{*0}(\Delta S = 2)$, the cross-feed effect is small even if we use the 90% upper limits to evaluate the cross-feed contribution to the yields. We do not correct for this contribution when extracting the upper limits.

There are several sources of systematic error. A substantial contribution comes from the uncertainty in track efficiency, which is 1.5% per charged track. For B decay modes with $K^{*\pm}$, there is an additional 5% uncertainty due to the K_S^0 vertex requirement. In addition, we estimate 1% per charged track uncertainty due to the dE/dx requirement. Additional systematic errors include 7% uncertainty from the thrust criterion and 3% from the ΔE and M_B requirements. Uncertainties due to Monte Carlo statistics range from 2% to 6%, depending on B decay mode.

The results of this analysis are summarized in Table I and displayed in Fig. 1; we see no statistically compelling signal in any individual decay channel. To calculate 90% confidence level (C.L.) upper limits on the number of signal events ($n_{u.l.}$) in each channel, we used a method based on the unified frequentist approach proposed by Feldman and Cousins [6] and adopted by the Particle Data Group [7]. We construct the confidence belts with 90% coverage using the likelihood ratio as the ordering principle for Poisson process when the total number of observed events n consists of signal events with mean n_S and background events with mean n_B :

$$P(n | n_S, n_B) = e^{-(n_S+n_B)} \frac{(n_S + n_B)^n}{n!}.$$

We assume that the background mean is not well known but fluctuates around the measured background $b = n_{b \rightarrow c} + n_{\text{off}}$ with Poisson probability and we summed over it:

$$P(n | n_S) = \sum_{n_B} P(n | n_S, n_B) e^{-b} \frac{b^{n_B}}{n_B!}.$$

To include the systematic error on the reconstruction efficiency we assume a normal probability distribution and convolute it with the $P(n | n_S)$ probability [8]. We also calculate the sensitivity of the experiment as the average signal upper limit that would be obtained by an ensemble of experiments with no true signal [6]. The upper limits on the branching ratios are then calculated from the formula

$$\mathcal{B}(B \rightarrow VV) = \frac{n_{u.l.}}{n_{B\bar{B}} \times \varepsilon \times \prod_B},$$

TABLE I. The 90% C.L. upper limits for the $B \rightarrow VV$ decay modes ($\mathcal{B}_{\text{CLEO}}$) are shown in units of 10^{-6} , along with the corresponding theoretical predictions ($\mathcal{B}_{\text{theory}}$) [3]. n_{obs} is the number of observed events, n_{off} is the off-resonance background (normalized), $n_{b \rightarrow c}$ is the $B\bar{B}$ background estimate (from Monte Carlo), $n_{u.l.}$ is the corresponding upper limit including systematic error and background statistics, and n_{sen} is the sensitivity of the measurement according to Feldman and Cousins' definition [6]. The reconstruction efficiency (ε) is also shown along with the systematic error ($\delta\varepsilon$).

Mode	Helicity	n_{obs}	n_{off}	$n_{b \rightarrow c}$	ε (%)	$\delta\varepsilon/\varepsilon$ (%)	$n_{u.l.}$	n_{sen}	$\mathcal{B}_{\text{CLEO}}^a$ ($\times 10^{-6}$)	$\mathcal{B}_{\text{theory}}$ ($\times 10^{-6}$)
$\rho^0\rho^0$	00	54	67	7.6	13	11	5.9	23	<18	0.54–2.5
	11				17	11			<14	
$K^{*0}\rho^0$	00	96	92	14	12	11	16	27	<34	0.7–6.2
	11				18	11			<24	
$K^{*0}K^{*0}$	00	22	14	1.6	11	11	18	11	<37	
	11				14	11			<29	
$K^{*0}\bar{K}^{*0}$	00	12	16	1.4	12	11	5.5	12	<22	0.28–0.96
	11				14	11			<19	
$K^{*+}\rho^0$	00	12	5.9	2.4	7.8	13	13	8.3	<74	0.8–14
	11				12	13			<49	
$K^{*+}\bar{K}^{*0}$	00	3	0.0	0.0	7.3	13	7.5	2.5	<71	0.29–1.8
	11				10	13			<48	
$K^{*+}K^{*-}$	00	0	2.0	0.0	6.6	17	1.5	4.6	<141	
	11				10	16			<89	

^a $\mathcal{B}_{\text{CLEO}}$ is calculated based on the sensitivity of the measurement (n_{sen}) instead of the signal upper limit ($n_{u.l.}$) if $n_{\text{sen}} > n_{u.l.}$.

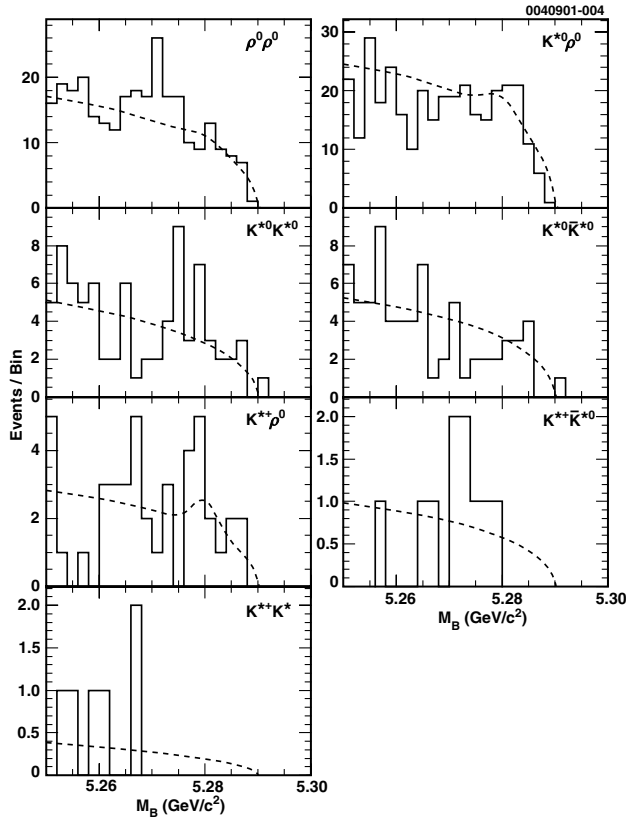


FIG. 1. B meson mass distributions for the seven modes discussed in the text. The histograms represent the data and the dashed lines represent the Monte Carlo prediction for the continuum plus $B\bar{B}$ background.

where $n_{B\bar{B}}$ is the number of $B\bar{B}$ meson pairs in the data sample, and \prod_B is the product over all the relevant branching fractions of the vector meson decay chain. We assume equal branching fractions for $\Upsilon(4S) \rightarrow B^0 \bar{B}^0$ and $B^+ B^-$.

To summarize, we set 90% C.L. upper limits on branching fractions of seven $B \rightarrow VV$ charmless decay modes. Theoretical predictions for the branching fractions of these modes tend to be near 10^{-6} . Thus our results are consistent with theoretical calculations based on the standard model. In order to challenge these predictions data samples of the order of $10^8 B\bar{B}$ mesons would be required.

-
- [1] D. Atwood and A. Soni, Phys. Rev. D **59**, 13 007 (1999).
 - [2] CLEO Collaboration, D. Cronin-Hennessy *et al.*, Phys. Rev. Lett. **85**, 525 (2000); CLEO Collaboration, S. J. Richichi *et al.*, Phys. Rev. Lett. **85**, 520 (2000); CLEO Collaboration, R. Godang *et al.*, Phys. Rev. Lett. **80**, 3456 (1998); CLEO Collaboration, B. Behrens *et al.*, Phys. Rev. Lett. **80**, 3710 (1998); CLEO Collaboration, T. Bergfeld *et al.*, Phys. Rev. Lett. **81**, 272 (1998); CLEO Collaboration, D. M. Asner *et al.*, Phys. Rev. D **53**, 1039 (1996).
 - [3] A. Ali, G. Kramer, and C.-D. Lü, Phys. Rev. D **58**, 94009 (1998); A. Deandrea *et al.*, Phys. Lett. B **320**, 170 (1994); N. G. Deshpande, in *B Decays*, edited by S. Stone (World Scientific, Singapore, 1994); D. Du and Z. Xing, Phys. Rev. D **48**, 4155 (1993); L. Chau *et al.*, Phys. Rev. D **45**, 3143 (1992); G. Kramer and W. F. Palmer, Phys. Rev. D **46**, 2969 (1992); M. Bauer, B. Stech, and M. Wirbel, Z. Phys. C **34**, 103 (1987).
 - [4] CLEO Collaboration, Y. Kubota *et al.*, Nucl. Instrum. Methods Phys. Res., Sect. A **320**, 66 (1992).
 - [5] G. Fox and S. Wolfram, Phys. Rev. Lett. **41**, 1581 (1978).
 - [6] G. J. Feldman and R. D. Cousins, Phys. Rev. D **57**, 3873 (1998).
 - [7] Particle Data Group, D. E. Groom *et al.*, Eur. Phys. J. C **15**, 1 (2000).
 - [8] R. D. Cousins and V. L. Highland, Nucl. Instrum. Methods Phys. Res., Sect. A **320**, 331 (1992).